Mineral characterization as a tool in the implementation of geometallurgy into industrial mineral mining

Aleksandra Maria Lang, Kurt Aasly, Steinar Løve Ellefmo
Norwegian University of Science and Technology, Department of Geoscience and Petroleum
Sem Sælands veg 1, 7491 Trondheim,
Norway

Corresponding author: aleksandra.lang@ntnu.no

Abstract

Industrial minerals play an important role in the Norwegian mining industry. The presented research focuses on defining marble deposit variability in order to evaluate parameters that can potentially be related to downstream process performance. Two types of marble raw material (K2 and K5) from the Verdalskalk open pit, used for precipitated calcium carbonate production (PCC) were tested for possible differences within texture, grain boundaries shape, grain size, accessory mineral assemblage. Additionally, surface hardness was measured using the Proceq Equotip D device. K5 type was found to be finer-grained compared to K2. The presence of quartz was more pronounced in K2 type material, which possessed higher surface hardness values and presented higher variation of those.

Keywords: Industrial minerals, Roasting, Process control

Introduction

With growing needs for ores and industrial minerals it has become essential to aim at constant improvement in recognition of the deposits and commodities not only in the geological but also mineral processing sense.

Chemical analysis and geological mapping are the main tools used to classify the raw material into different types and qualities. The presented study aims to recognize, describe and quantify mineralogical and textural properties of a calcite marble deposit and define parameters that can be used for qualifying the deposit into different geometallurgical domains.

The specific objectives of this research are:

- to describe and compare the mineralogical and textural properties of two types of marble used for Precipitated Calcium Carbonate (PCC) production
- to present and compare surface hardness test results for both types of marble
- to define potential links between surface hardness values and the mineralogical and textural properties
- to verify the appropriateness of the Equotip D as a portable time- and cost efficient geometallurgical test tool for surface hardness in marble deposits.

Background

The Tromsdalen deposit operated by Verdalskalk AS is located in Mid-Norway. The deposit, being low metamorphic grade calcite marble of the Ordovician period, is estimated to be 7.5 billion tonnes. The marble unit is situated between greenschist and phyllite units (Figure 1, left). Due to folding the units occurs in reverse order, with greenschist situated on top the marble and phyllitic strata laying underneath (Gautneb, 2012).

The Tromsdalen marble is fine to medium grained, greyish with lighter and darker bands (Figure 1, right). The typical marble is relatively pure. Most common impurities for Tromsdalen marble are iron oxides, iron sulfides and silicate minerals. Graphite, pyrite, quartz, pyroxene, muscovite and apatite are typical for carbonate rocks (Korneliussen et al., 2014).

A

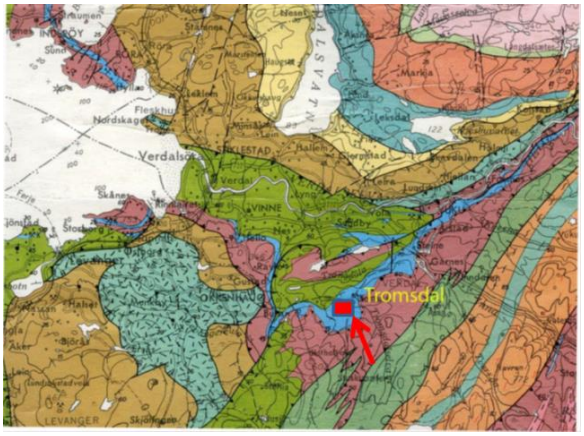

B

Figure 1: Geological overview of the Tromsdalen area (A); The marble unit (blue) is located between greenschist to SE (violet) and phyllite to NW (green) (Gautneb, 2012). Typical Tromsdalen marble (B).

The marble is mined in an open pit operation. Based on chemical data as well as physical appearance (color), the deposit is subdivided into 6 marble types (Table 1). The types are assigned to production qualities based on the CaO, Fe_2O_3, SiO_2 and Al_2O_3 content. XRF analysis control is performed on drill cores, drill chips and along production line.

The A (pure) quality consists of types K1, K2 and K5 and is used as raw material for the burned and slaked lime production. The blasts consisting of blended pure and impure marble (e.g. K2 and K3) are classified as B (standard) quality and used as feed to a kiln operated by a different company with lower purity standards. The lower purity K3 and K4 type raw material is used for cement production (C quality). Type K6 occurs as a thin strata on a contact with a greenschist unit and is not utilized in production due to high impurity levels (Ruiz J.R., pers.com, 06.03.2015).

The raw material of pure quality is crushed and screened at the mine site before it is transported by truck to the kiln, where it is converted to quicklime (burned lime, CaO), which is the main product from the mine. The CaO is used for PCC production. The crushing plant at the mine site consists of roller crushers with primary and secondary crushing lines. Crushed products are screened to the 30-100 mm fraction, which is then fed to the kiln. At Verdalskalk the calcium oxide is produced in a two-shaft Maerz kiln due to the reaction:

$\mathbf{CaCO_3 + Heat \rightarrow CaO + CO_2 \uparrow}$,in temperatures reaching 1000-1200 C° in the burning zone (Storli, A.M., pers.com, 07.03.2015).

Table 1: Quality requirements for marble types in Tromsdalen deposit

Type no.	Name	Quality requirements		
		CaO (wt%)	Fe_2O_3 (wt%)	SiO_2 (wt%)
K1	Light-grey pure marble	>54,5	<0,06	<0,5
K2	Dark-grey pure marble	>54,5	<0,06	<0,5
K3	Dark-grey impure marble	>50,0	>0,12	No requirements, given the purity of the deposit
K4	Light-grey impure marble	>50,0	>0,12	
K5	Black marble, pure	>54,5	<0,06	<0,5
K6	White marble, impure	Waste material, no requirements		

Currently, marble types K2 and K5 are fed directly to the kiln. They both are of equally high purity but there is an indication, based on operator experience, that marble type K2 has less stable processing performance in the kiln than marble type K5. With similar geochemical data between marble types K2 and K5, there is a need for understanding which mineralogical parameters other than bulk geochemistry influence the kiln performance.

Hence it is reported (Boynton, 1966) that grain size differences can cause changing of the calcite heating pattern in the kiln, as coarse grains tend to crack instead of dissociate, therefore this parameter should be taken into account when classifying raw material into processing types.

The current research is a part of the project aiming at incorporating the aspects of geometallurgy into industrial mineral operations. Typically, geometallurgy is used in metal mining. However, it can be also used for better recognition of process performance and quality needs within industrial minerals.

The main goal of this study is to define new key performance indicators (KPIs) within industrial mineral mining, establishing the links between them and "traditional" indicators such as chemistry, and searching for geometallurgical tests that are suitable for industrial minerals operations. Lischuk et al. (2015) described two main approaches to establish the links utilized in geometallurgy: the mineralogical approach and geometallurgical tests. In the presented research both approaches were applied: mineralogical characterization of the commodity was performed and s surface hardness test was examined as potential geometallurgical testing method.

Materials and methods

Materials:

Mineralogy

The sampling campaign for the microscopic study was performed in the Tromsdalen calcite marble deposit in the blast piles after production blasting.

Material from four production blasts, VB11-2016, VB13-2016, VB16-2016 and VB19-2016 was tested and 9 samples were collected from each blast (Table 2). In order to test potential variabilities of the marble within mostly homogenous blasts the samples were collected along

the pile and the emphasis was on collecting samples that showed visual variations. The distribution of the samples along the blasts is illustrated in Figure 2.

Blasts of two different marble types – K2 and K5, both used as a raw material for the kiln, were selected for the study.

Table 2: Sample numbers with corresponding blast number and marble type

Sample signature	Production blast	Sample signature	Production blast	Marble type
1-VB11	VB11-2016	1-VB16	VB16-2016	K2
2-VB11		2-VB16		
3-VB11		3-VB16		
4-VB11		4-VB16		
5-VB11		5-VB16		
6-VB11		6-VB16		
7-VB11		7-VB16		
8-VB11		8-VB16		
9-VB11		9-VB16		
1-VB13	VB13-2016	1-VB19	VB19-2016	K5
2-VB13		2-VB19		
3-VB13		3-VB19		
4-VB13		4-VB19		
5-VB13		5-VB19		
6-VB13		6-VB19		
7-VB13		7-VB19		
8-VB13		8-VB19		
9-VB13		9-VB19		

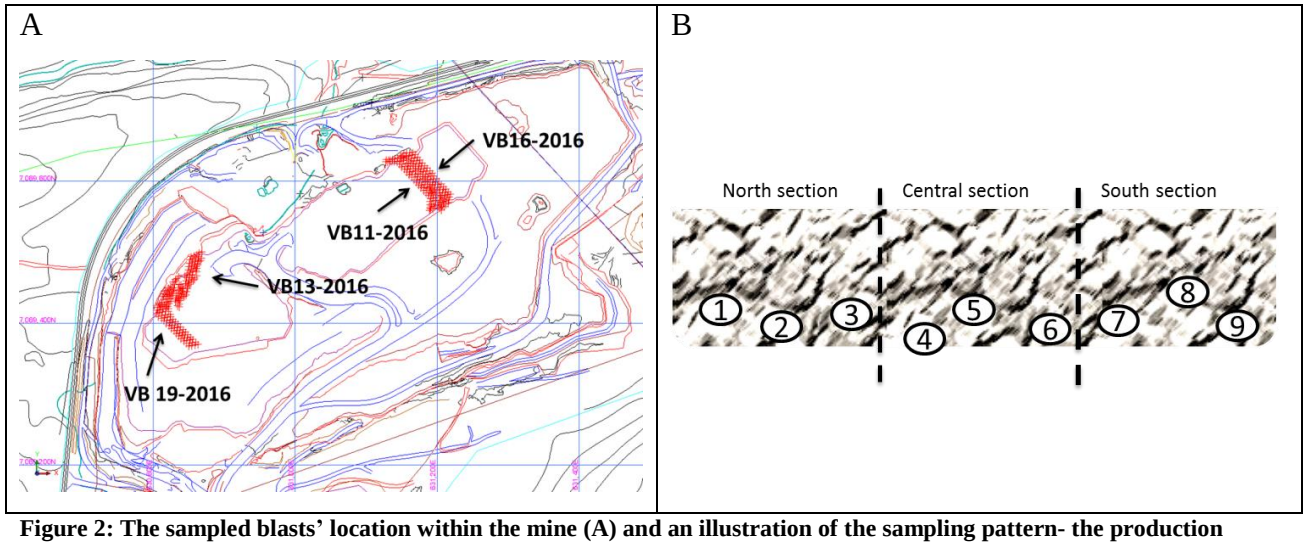

Figure 2: The sampled blasts' location within the mine (A) and an illustration of the sampling pattern- the production blasts was divided into three parts and three samples were taken from each part (B).

Surface Hardness

For the surface hardness measurements, the sampling areas were selected among the largest, stable blast fragments (Figure 4) and the measuring points were located on the most even surfaces with minor topography and fractures, and with the least trace of weathering and alteration.

A total amount of 110 sample surfaces from 10 separate blasts were tested (Table 3).

Table 3: Surface hardness measurements: Chosen production blasts and number of surfaces tested. Note that blast VB16-2015 is split into three parts due to the large dataset.

Blast number	type	Amount of results (tested surfaces)
VB15_2015	K5	18
VB16a_2015		10
VB16b_2015		10
VB16c_2015		10
VB17_2015		7
VB21_2015		6
VB13_2016		9
VB19_2016		9
VB20_2015	K2	6
VB11_2016		10
VB16_2016		12
VB17_2016		3

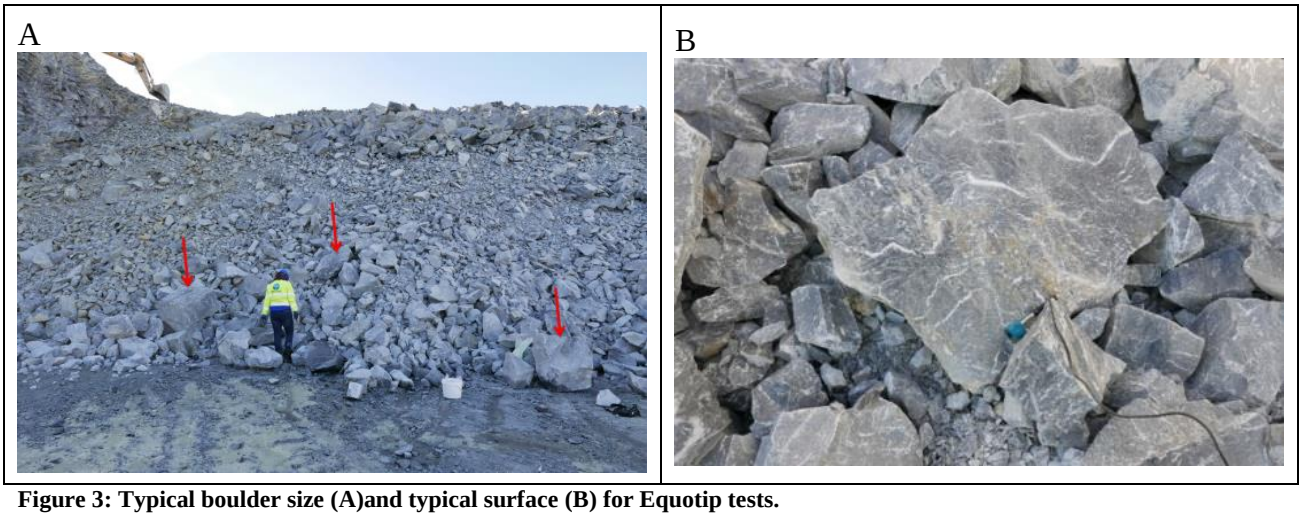

Figure 3: Typical boulder size (A)and typical surface (B) for Equotip tests.

Methods:

Mineralogy

One polished thin section was prepared from each rock sample. The samples were cut perpendicularly to existing foliation and thin sections were prepared at the Warsaw University (UW).

The petrographic and mineralogical investigations of the thin sections were conducted at the Norwegian University of Science and Technology (NTNU) in Trondheim. A Nikon Eclipse 600 polarized light microscope with a 2 MP digital optical camera was used to record transmitted and reflected light observations. Grain measurements were performed manually using SPOT software. The equivalent circle diameters were measured and the typical grain size within a thin section was estimated based on this. A Scanning electron microscope (Hitachi SU-6600 LV-FE-SEM with Bruker XFlash detector) was applied to chosen thin sections to identify the minerals by backscattered electron imaging (BSE) and energy dispersive X-ray spectroscopy (EDS), with use of Bruker Quantax Esprit software. MinDat website was used to confirm mineral ID and composition.

Surface Hardness

The blasted material from the ten blasts was tested for surface hardness using a rebound hardness tester. In the test conducted by a Proceq Equotip 3 D device the impact body is propelled by spring force against the tested specimen. Surface deformation results in energy loss, which is detected by measuring and comparing the velocities of the impact body in both impact and rebound phases. The hardness value is expressed as the Leeb Number (*L*value) or Leeb Hardness (HL), which is the ratio of the rebound velocity to the impact velocity multiplied by 1000 (Viles et al., 2011). Surface hardness tests require that the tested surface is smooth and even, and that the specimen is heavy and stable. The single impact method (Aoki and Matsukura, 2007, Viles et al., 2011) was modified for this research: Each sample surface was tested with 10 measurements in random locations on the surface and for each surface the resulting L_{max} value was calculated as an average from the 3 highest readings.

The original method by Aoki and Matsukura proposes a set of 20 readings per surface. However, the present research was conducted under field conditions and the even and smooth surfaces were not always large enough to conduct 20 measurements. For the same reason, there was a high chance of error readings, and therefore the authors decided to reduce the amount of readings from 20 to 10, and reduce the amount of valid readings to the three highest, assuming that an Equotip reading cannot be too high, but can be lowered due to the surface not being perpendicular to the force vector. Hence, the only possible mistakes are lower values rather than higher values.

For the blasts VB11-2016, VB13-2016, VB16-2016 and VB19-2016 the sampling areas were following the mineralogical sampling pattern (Figure 2).

Results

Mineralogy

Calcite was the major mineral in all samples. The typical grain size of all samples was within a range of 50 – 400 μm (Figure 4A, B, Figure 5). In most of the samples porphyroblasts (recrystallized calcite grains) were surrounded by a rim of micro- and cryptocrystalline calcite less than 10μm in size.

Almost all samples presented heteroblastic (recrystallized calcite grains were of different size within a thin section) texture (Figure 4C). Heteroblasticity was a summary of two factors: microcrystalline calcite grains and coarse veins/layers.

The microcrystalline fraction was usually pronounced as rims between porphyrooblasts boundaries but the amount of this, as well as the size range of this fraction varied from sample to sample and could vary considerably within a sample.

Grain boundary shape was similar for all samples and was typically a combination of curved, slightly sutured, embayed and straight grain boundaries, in different proportions. The straight triple junction grain boundaries characteristic for fully recrystallized calcite were not abundant in any sample.

Accessory minerals found in thin sections were typically pyrite, graphite, iron hydroxides and quartz. It is important to note that within all thin sections total impurities constituted less than 1% of the mineralogy.

Pyrite was the most common impurity mineral and occurred typically as sparse euhedral inclusions within calcite porphyroblasts – in most of the samples (figure 4D), or as framboidal aggregates associated with graphitic layers- mostly in samples related to the blast VB19-2016 (Figure 4F). In most of the samples pyrite crystals were less than 20μm across.

Mineral iron oxide was present mostly as a pseudomorph after pyrite, of typical pyrite shape (Figure 4D) but irregular elongated grains were also observed.

Silica minerals observed in the samples were quartz and muscovite. The typical size of quartz grains ranged between 50 and 100μm (figure 4E).

Four of the samples were additionally observed under SEM, and EDS analysis was conducted. Additionally to minerals mentioned above, micro grains of apatite and TiO_2 were detected.

For compiled mineralogical and petrographic results see appendix A.

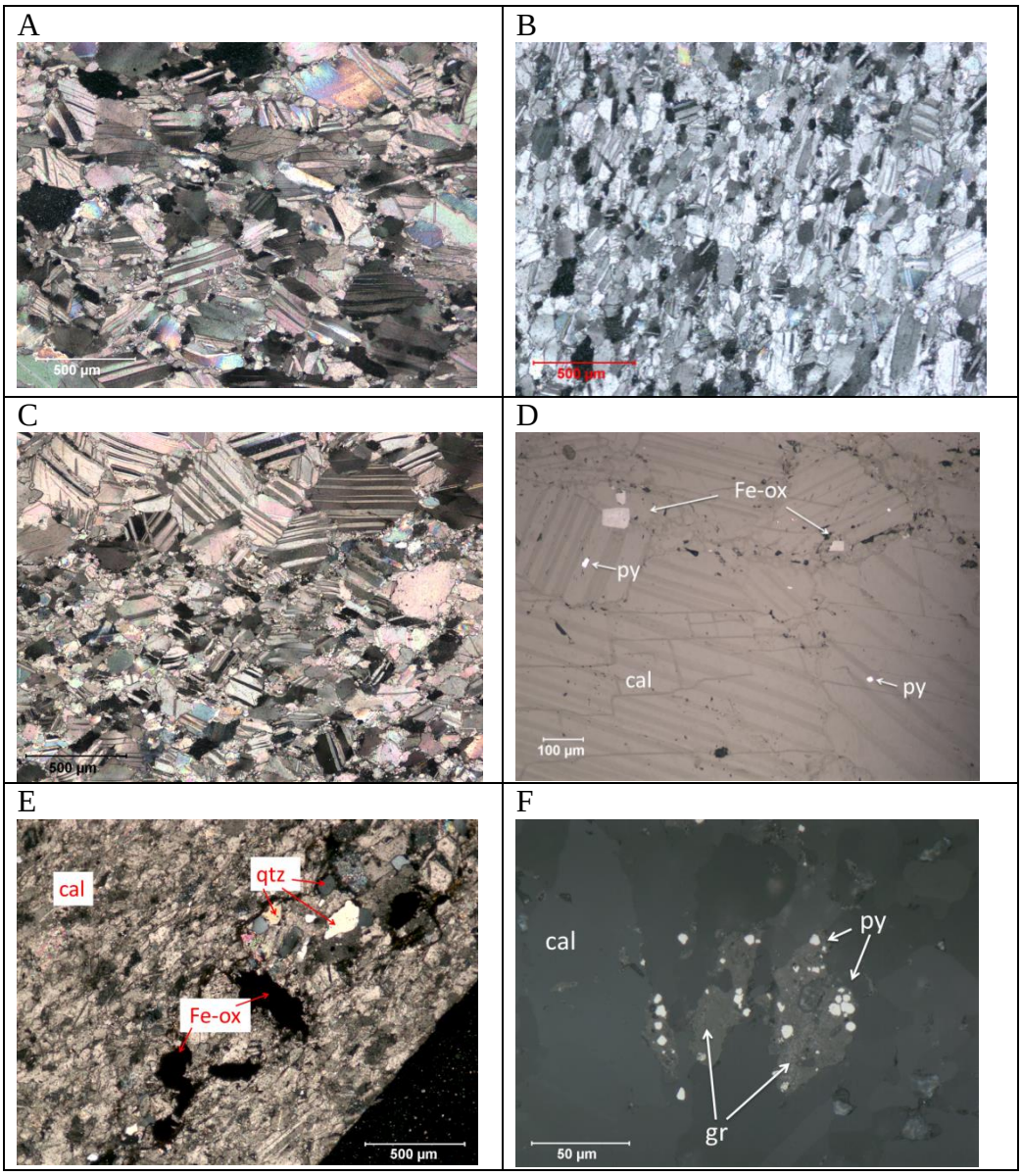

Figure 4: A: Microphotograph in cross-polarized light, sample 2-VB16, coarse grained with micro- and cryptocrystalline calcite located on boundaries. B: sample 2-VB13. Porphyroblasts much smaller, microcrystalline calcite present, but less pronounced. C: sample 8-VB13, example of extremely heteroblastic calcite, typical grain size impossible to estimate. D: sample 9-VB11, reflected light. Pyrite grains and Fe-ox pseudomorphs after pyrite. E Sample 5-VB11, cross polarized light. Quartz and Fe-ox grains surrounded by microcrystalline calcite matrix. F: sample 9-VB13, reflected light. Framboidal pyrite inclusions in graphite. The mineral abbreviations: cal- calcite, py – pyrite, qtz – quartz, gr – graphite

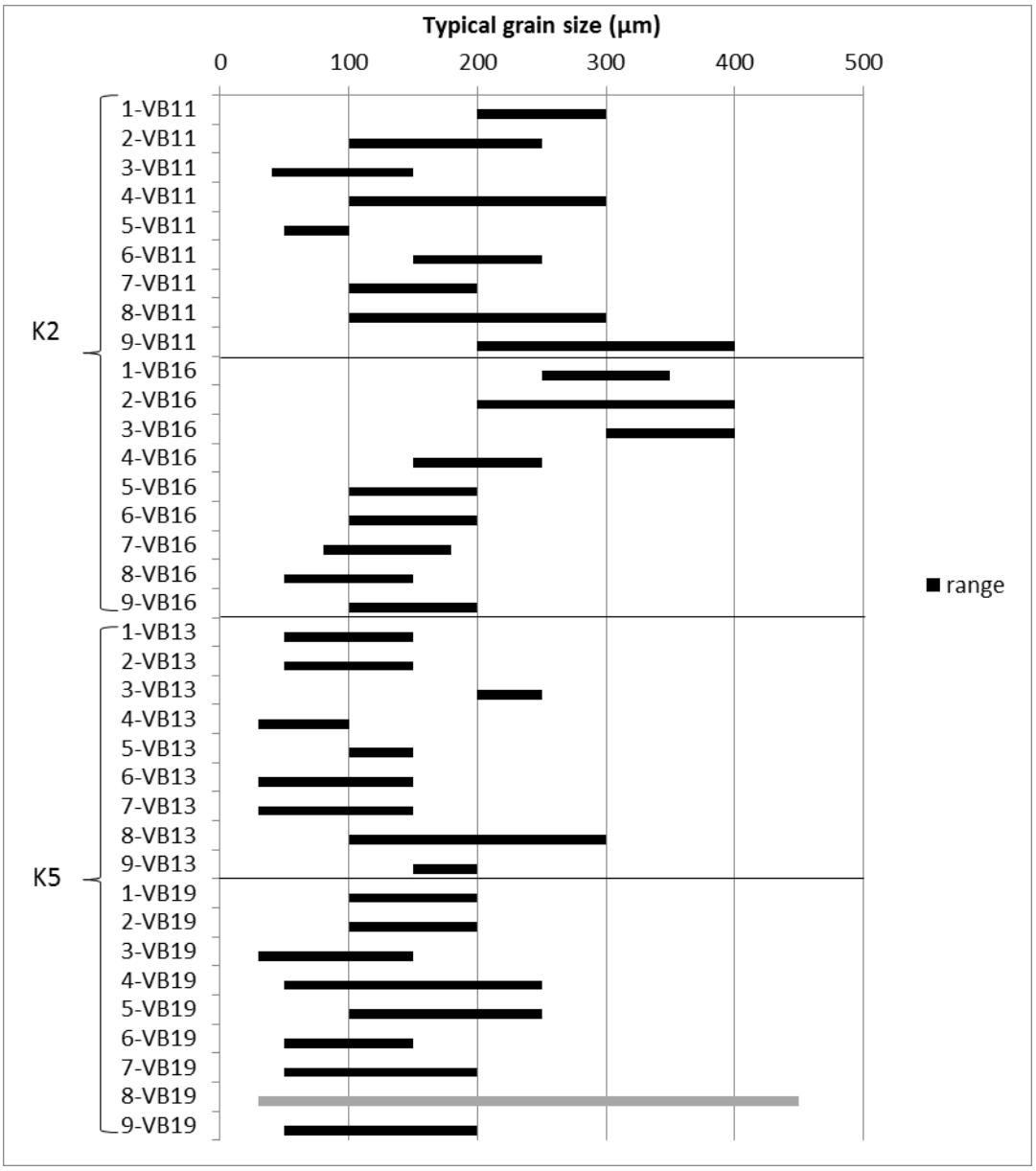

Figure 5: Typical grain size (equivalent circle diameter, µm) of each thin section. Note that for the thin section 8-VB19 it was not possible to estimate the typical grain size, as the range was too broad.

K2 marble type

Within production blast VB11-2016 typical porphyroblast size varied between 50 and 400µm in total. Porphyroblasts of less than 100µm were typical for two thin sections, and porphyroblasts larger than 250µm were typical for four thin sections. In sample 9-VB11 grains bigger than 400µm were present. Thin sections from production blast VB16-2016 showed similarities to those of blast VB11 and were generally coarse grained. In four out of nine thin sections the typical size range exceeded 200µm, and in two of the thin sections was lower than 100µm.

Almost all samples presented heteroblastic texture, and the texture was locally homeoblastic for samples 6-VB16 and 8-VB16.

Microcrystalline and cryptocrystalline grains were mostly pronounced in samples 1-VB11, 9-VB11, 1-VB16, 2-VB16, 3-VB16. In sample 3-VB11 and sample 5-VB11 porphyroblasts were surrounded by a matrix of microcrystalline calcite that was the main constituent of the sample.

Pyrite was found in almost all samples of K2 type. In most of the samples pyrite crystals were less than 20μm across. In sample 2-VB11, 6-VB11, 2-VB16 pyrite was very sparse and in sample 9-VB11 and 7-VB11 was absent.

Iron oxide mineral was found in five samples within blast VB11-2016, six samples of blast VB16-2016. In sample 9-VB11 Fe-ox was most abundant and the grains were up to 100μm.

Graphite elongated aggregates and layers were observed in one sample of VB11-2016

Quartz grains were observed in five samples of the blast VB-11-2016 and two samples of the blast VB16-2016. The typical size of quartz grains ranged between 50 and 100μm (figure 8E).

Muscovite was observed in sample 7-VB11.

K5 marble type

Within blast VB13-2016 typical grain size varied from <50 to 200μm .For three of the thin sections the typical size was less than 100μm, and for one thin section typical grain size was larger than 250μm.

Thin sections obtained from the VB19-2016 blast were generally fine-grained, for five out of nine sections the range of typical grain size comprised value lower than 100μm, but contrary to other blasts, in this set of samples the veins of coarse to very coarse material were present. In sample 7-VB19 only one coarse grained vein was visible, with calcite porphyroblasts of sizes up to 3 mm. In thin slip 9-VB19 there were several veins of coarse calcite, whereas in thin slip 2-VB19 there were several transitions from the coarser grained areas to finer grained areas. Thin section 8-VB19 presented extremely heteroblastic texture with extensive microcrystalline occurrence as well as many areas of coarse material.

Microcrystalline and cryptocrystalline grains were mostly pronounced in thin sections from samples 6-VB13, 7-VB13, and most of the thin sections from blast VB19-2016.

Pyrite was the found in all K5 type sections. Pyrite occurrence as framboidal aggregates associated with graphitic layers was visible in thin slips related to the blast VB19-2016.

Iron oxide was noted in four thin sections within blast VB13-2016 and five sections of blast VB19-2016.

Graphite elongated aggregates and layers were observed in one thin section of VB13-2016 blast, and most extensively, in thin slips representing the blast VB19-2016.

Quartz grains were observed in one thin section of the blast VB-13-2016 and none of the blast VB19-2016. For comparison of accessory minerals between marble types see Figure 7.

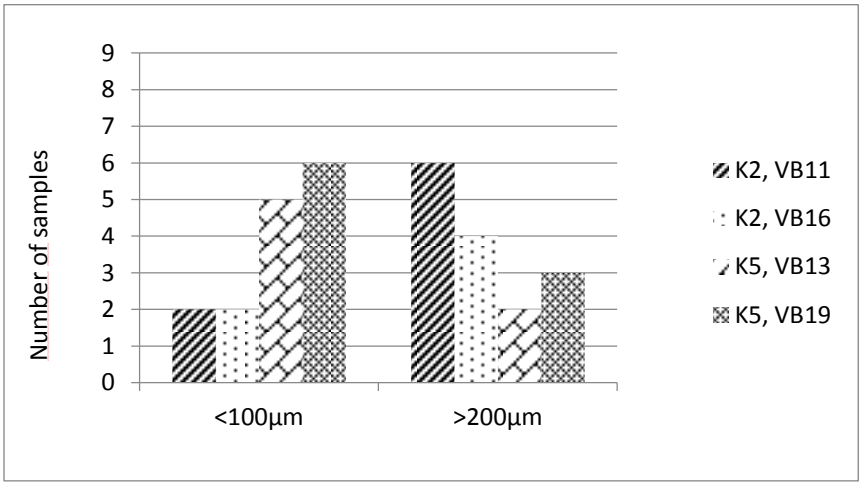

Figure 6: Comparison of grain sizes observed in thin sections. The figure shows the number of thin sections per blast in which typical grain size is within a range of less than 100 and more than 200 µm respectively.

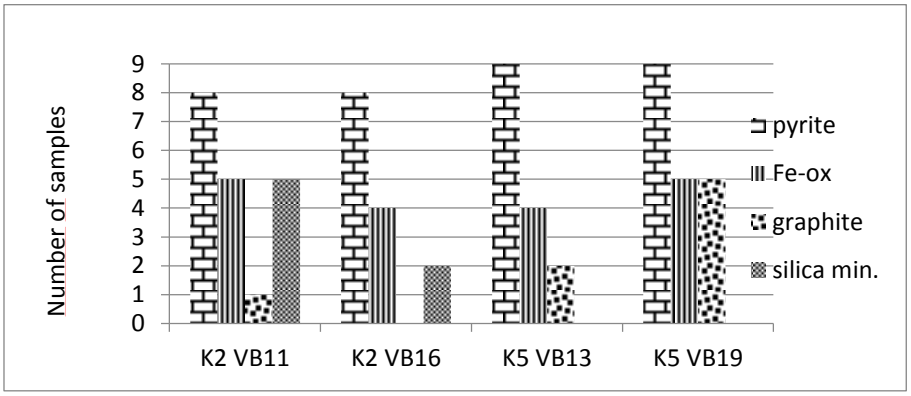

Figure 7: Comparison of accessory minerals observed in thin sections from each blast. Note that silica was only observed in type K2 marble, while most graphite was observed in K5 type.

Surface Hardness

The calculated L_{max} values of the surface measured oscillated between 480 and 650.3 HLD (Figure 10, Figure 9).

The average L_{max} values of blasts were relatively similar for each of the production blasts and oscillated between 530.4 HLD and 577 HLD (Table 4).

The standard deviation of each blast's measurements oscillated between 23.0 and 48.3 (Table 4, Figure 8).

The measurement uncertainty of each L_{max} value, that is standard deviation of the 3 readings that constitute the value, was also calculated. The results were shown in Figure 9 as error bars attached to each L_{max} value point. The average measurement uncertainty per blast was also calculated (Table 4 and Figure 9) and they ranged between 14.2 and 25.7.

K5 marble type

The majority of the surfaces tested belonged to the K5 type due to better accessibility in the pit during sampling campaigns. The calculated L_{max} values were between 478 and 618 HLD.

The standard deviation of L_{max} measurements per blast oscillated between 23.0 and 40.4. The most homogenous measurements were noted for the central part of VB16-2015 (VB16b-2015). The average measurement uncertainty of production blasts oscillated between 15.1 and 25.7. The highest average measurement uncertainty obtained (25.7) was noted for the blast VB13-2016.

K2 marble type

For the type K2 the L_{max} value oscillated between 486.3 and 650.3. The three highest L_{max} values of entire campaign were noted for blasts VB11-2016 and VB16-2016.

The blasts standard deviation oscillated between 28.3 and 48.3which was the highest value obtained.

The average measurement uncertainty was within a range of 14.2 and 23.4 and the lowest uncertainty obtained in the results (14.2) was noted for the blast VB20-2015.

Table 4: Average L_{max} values and standard deviation (st dev) presented per blast.

Blast number	Type	Average L_{max}	St. dev.	Av. of single value st.dev.
VB15_2015	K5	551,4	29,3	24,3
VB16a_2015		573,4	29	18,8
VB16b_2015		577,3	23	15,1
VB16c_2015		553,7	24,7	18,4
VB17_2015		564,5	32,9	23,9
VB21_2015		567,7	33,4	20,6
VB13_2016		559,6	40,4	25,7
VB19_2016		569,8	23,4	19,5
VB20_2015	K2	543,9	32,4	14,2
VB11_2016		566,4	48,3	19,5
VB16_2016		564,4	44,8	23,4
VB17_2016		530,4	28,3	22,3

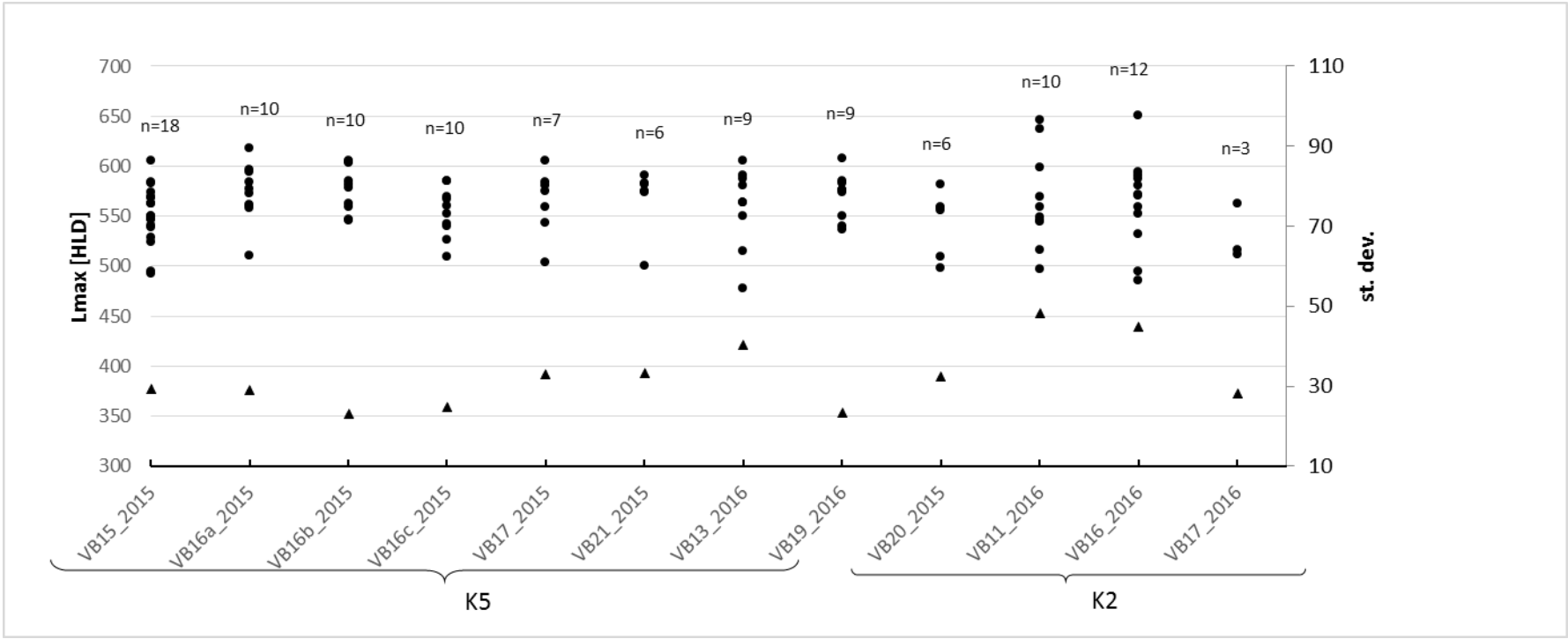

Figure 8: Equotip tests results. Dots refer to the left hand axis and present L_{max} values for each blast. Triangles refer to the right hand axis and represent the standard deviation of results for each blast.

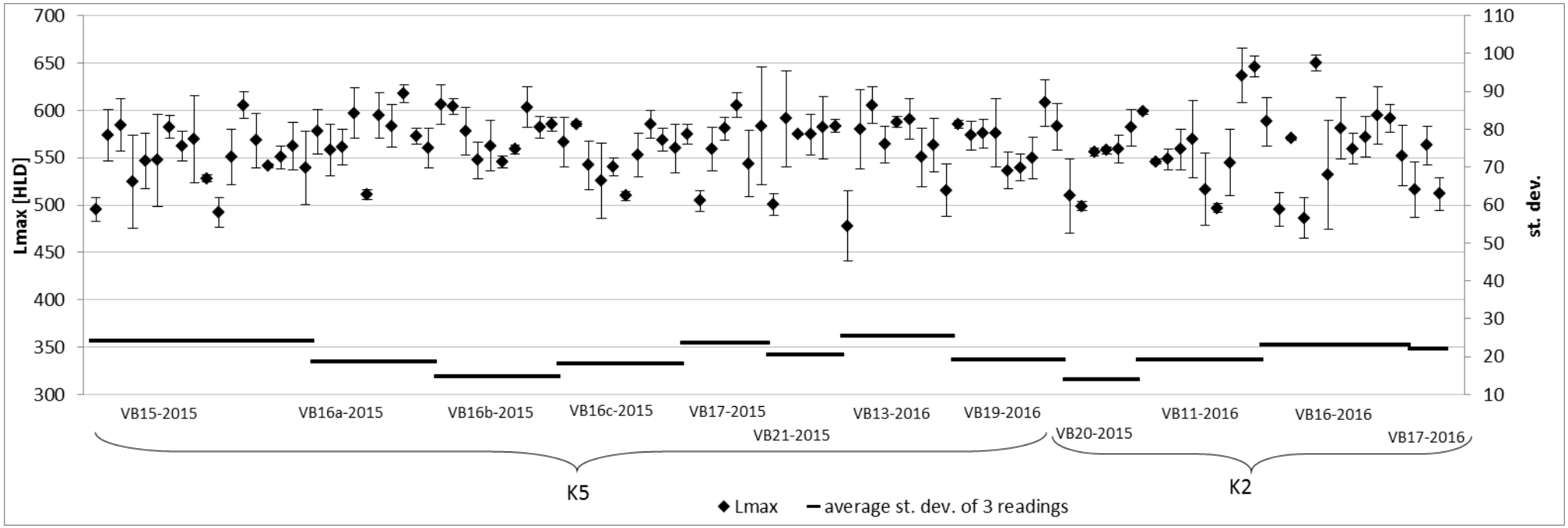

Figure 9: Equotip tests results. The left hand axis refers to the L_{max} values for each blast. Error bars attached show the measurement uncertainty (based on standard deviation of the 3 Equotip readings included in the final L_{max} value). The right hand axis refers to the average measurement uncertainty of each blast and is shown as thick lines.

Discussion

Mineralogy

It was observed that the type K2 thin sections were in general coarser grained than those of type K5 and for K5 type the fine grained calcite of less than 100um was more typical (Figure 6). However both types had variations in grain size. While for the K2 type the variation was mostly between coarse and very coarse grains, the K5 type presented both very fine and very coarse grain size, especially in the blast VB19-2016.

Microcrystalline calcite located in-between porphyroblast boundaries was generally pronounced in both types of marble, but blast VB19-2016 contained the most abundant micro- to cryptocrystalline fraction.

As stated by Boynton (1966), the grain size has a major impact on the heating pattern in the kiln, and this raises a need for redefining the marble types at Verdalskalk in order to take into consideration the differences in calcite grain size and divide the current K5 type into subtypes.

Pyrite was present in both types of marble. It was observed in different forms (euhedral, anhedral, disseminated and aggregated) but no trends were observed in terms of changing abundance between marble types.

The type K5 marble has been reported by the company to have higher a graphite content, hence the colour and name of the type (Table 1). The graphite grains were reported to be very fine grained and disseminated (Gautneb, 2012). In the present research however, visible graphite grains were most pronounced in the VB19-2016 samples. It is suggested that higher graphite content may cause different heating patterns locally as the graphite burns prior to the calcium dissociation because of the differences in the combustion enthalpies (-393,5 kJ/mol for graphite, vs 177,8 kJ/mol for calcite (Rodriguez-Navarro et al., 2009).

The presence of silica minerals was more noticeable in type K2 material as there were seven samples containing quartz and one containing muscovite, compared with only one sample containing quartz within type K5. It is highly possible that silicate minerals which were more abundant in type K2 can make the raw material behave slightly differently in the kiln by forming dicalcium silicate layers (Hökfors, 2014). Therefore even if the overall amount of silicate minerals in the kiln is below the cut-off value, the need for redefining the cut-off value in the future or the need for examining the raw material more locally before processing in the kiln may arise.

Surface Hardness

The Equotip D device was tested as a potential tool for easily-accessible, portable, low-cost geometallurgical testing. The method of testing blocks of raw material instead of drill cores was applied. Overall results were similar for both types of marble and did not vary from type to type in terms of average L_{max} value of production blast. Single measurements however, showed variations and it is important to note that the 3 highest L_{max} values were obtained for the K2 type.

All the results showed differences in terms of standard deviation – within a blast as well as within a single L_{max} value (measurement uncertainty).

Varying standard deviation is an indicator that some parts of the deposit have less homogenous internal structure. In terms of a blast standard deviation, the highest value was noted for K2 type and lowest for K5 type, but in terms of a single surface average standard deviation the highest value was noted for K5 type and the lowest for K2 type. It can be an indication of the different scale of internal variability of the raw material: while high standard deviation of a blast shows that measurements differed from surface to surface (in different parts of a blast), the high values within a surface represent the variability within a single surface, that is, on a smaller scale.

Relation between mineralogy and surface hardness values

Two process implications of raw material parameters can potentially be interpreted from the Equotip measurements. 1) L_{max} values represent the internal textures of the calcite and hence, can be used as proxy for mineralogical textures 2) L_{max} values may be used as a proxy for crushing hardness and the final particle size distribution from the crusher (Montoya, 2014). Both parameters are known to have influence on furnace performance as stated by Boynton (1966).

The collected data allowed for comparison between mineralogy and the Equotip testing results for blasts VB11-2016, VB13-2016, VB16-2016 and VB19-2016. It is important to note that the link between the results is not direct, as the samples used for thin sections were located in similar places within a blast, but were not the same as the surfaces used for the Equotip testing.

For K2 type it appears that the high L_{max} values obtained in blasts VB11-2016 and VB16-2016 are related to the coarser grain size and possibly higher silica content. The blast VB11-2016 was observed to have larger variation in terms of grain size which appears to be followed by higher standard deviation of surface measurements in the blast (Figure 8).

However, the blast VB16-2016 reached higher average value of the measurement uncertainty (Figure 9) and therefore, this might be an indication of a smaller scale variability comparing to blast VB11-2016. An example would be small scale quartz veinlets compared to thick layers of coarser calcite within a blast.

Relation between mineralogy and L_{max} values in K5 type is more difficult to establish. The Equotip measurements show that both on a scale of single surface (Figure 8) as on a scale of single measurement (Figure 9), the standard deviation is higher for blast VB13 than VB19, which seems to be contrary to mineralogical observations (Figure 5) where blast VB13 tended to be more homogenous in terms of grain size. The abundance of accessory minerals is also lower for blast VB13-2016 than for the blast VB19-2016 (Figure 7). Hence, the reason for more homogenous L_{max} results in VB19-2016 is interpreted to be related to higher content of microcrystalline calcite which is an indication of higher level of metamorphic recrystallization. More Equotip tests are required in order to establish the links between parameters.

Conclusion

This study showed significant differences between two marble types that to date have been processed as the same quality. Based on obtained results the following conclusions can be drawn:

- Thin sections of marble type K5 were generally more fine-grained than those of type K2
- Marble type K5 was however not homogenous in terms of grain size, as very fine and coarse grains coexisted within one blast samples

- Quartz was observed in thin section more often in type K2 samples than in type K5 samples

- Graphite was observed mostly in blast VB19-2016 belonging to K5 type.

- The grain size and mineralogical differences within marble types indicate the need for revision of the classifying parameters in order to establish new geometallurgical domains that could improve the process performance.

- The Equotip D measurements showed that K2 type samples reached higher L_{max} values than K5 samples and had more variability within certain blasts

- The K5 type material was on average more variable locally (within tested surfaces of certain blasts).

- Further Equotip D tests are needed in order to observe possible trends and relations to internal structure of the marble.

Further studies of marble textures via use of image analysis and marble behaviour during dissociation via the use of a heating stage microscope are planned for the next part of the research study.

Acknowledgement

This research is funded by the Research Council of Norway in the User-driven Research based Innovation (BIA) program under the grant agreement 236638/O30, the industry partners and the Norwegian University of Science and Technology.

References

AOKI, H. & MATSUKURA, Y. 2007. A new technique for non-destructive field measurement of rock-surface strength: an application of the Equotip hardness tester to weathering studies. *Earth Surface Processes and Landforms,* 32**,** 1759-1769.

BOYNTON, R. S. 1966. *Chemistry and technology of lime and limestone,* New York, Interscience.

GAUTNEB, H. 2012. Kommunedelplan Tromsdalen, Verdal. Oversikt over geologiske forhold, marked og produksjon av kalkstein.

HÖKFORS, B. 2014. *Phase chemistry in process model for cement clinker and lime production.* PhD, Umeå Universitet.

KORNELIUSSEN, A., RAANESS, A. & GAUTNEB, H. 2014. Chemical and mineralogical characterisation of carbonate deposits in Norway. *NGU Report*.

LISCHUK, V., LAMBERG, P. & LUND, C. 2015. Classification of geometallurgical programs based on approach and purpose. *SGA 2015.* Nancy.

MONTOYA, P. L. 2014. *Geometallurgical Mapping and Mine Modelling - Comminution Studies: La Colosa Case Study, AMIRA P843A.* Master of Science in Geology, University of Tasmania.

RODRIGUEZ-NAVARRO, C., RUIZ-AGUDO, E., LUQUE, A., RODRIGUEZ-NAVARRO, A. B. & ORTEGA-HUERTAS, M. 2009. Thermal decomposition of calcite: Mechanisms of formation and textural evolution of CaO nanocrystals. *American Mineralogist,* 94**,** 578-593.

VILES, H., GOUDIE, A., GRAB, S. & LALLEY, J. 2011. The use of the Schmidt Hammer and Equotip for rock hardness assessment in geomorphology and heritage science: a comparative analysis. *Earth Surface Processes and Landforms,* 36**,** 320-333.

Appendix

sample			Typical grain size (μm)	Grain Boundary Shape	Other textural features	Accessory Minerals
K2	VB11-2016	1-VB11	200-300	cu, em, su	m	py, Fe-ox
		2-VB11	100-250	cu, em, su		qtz, (py)
		3-VB11	<50-150			py, Fe-ox
		4-VB11	100-300	cu, str		py, Fe-ox
		5-VB11	50-100	cu, em	m cv 100-200 μm	qtz, py, Fe-ox *ap, Ti-ox*
		6-VB11	150-250	su, em		qtz, (py)
		7-VB11	100-200	cu, str, em		qtz, ms, py, gr
		8-VB11	100-300	su, em, sc		qtz, py
		9-VB11	200-400	cu, str, su	m	Fe-OX
	VB16-2016	1-VB16	250-350	cu, su, str	m	py, (Fe-ox)
		2-VB16	200-400	su, em	m	Fe-ox, (py)
		3-VB16	300-400	cu, su	m	qtz, py
		4-VB16	150-250	su, str, em		py
		5-VB16	100-200	cu, str, su		py
		6-VB16	100-200	cu, su		PY
		7-VB16	80-180	cu, str		qtz, (Fe-ox)
		8-VB16	50-150	cu, su, str	cv 350-600μm	py, Fe-ox
		9-VB16	100-200	cu, su, str		py-Fe-ox

sample			Typical grain size (μm)	Grain Boundary Shape	Other textural features	Accessory minerals
K5	VB13-2016	1-VB13	50-150	cu, str, su	m	py, Fe-ox
		2-VB13	50-150	str, cu	m	py
		3-VB13	200-250	su, em, cu		py, Fe-ox *Ti-ox*
		4-VB13	<100	cu		py, gr
		5-VB13	100-150	cu, em, su		py, Fe-ox
		6-VB13	<150	cu, su	m	py
		7-VB13	<150	em, su	m	PY
		8-VB13	100-300	cu, str		qtz, py, Fe-ox
		9-VB13	150-200	cu, str	m	py, gr
	VB19-2016	1-VB19	100-200	su, cu	m	py, gr, Fe-ox
		2-VB19	100-200	su, em	m	py, gr, Fe-ox
		3-VB19	<150	su, cu	m, cv 350-600 μm	py, gr, Fe-ox
		4-VB19	50-250	su, em		(py)
		5-VB19	100-250	su, cu		(py)
		6-VB19	50-150	su, cu	m, cv 300-450 μm	(py)
		7-VB19	50-200	str, cu	cv 3mm	py, gr, Fe-ox
		8-VB19	0-450	su, cu, em	m	py
		9-VB19	50-200	su, cu, em	cv 300 μm	py, gr, Fe-ox

Appendix A: Compilation of information for mineralogical samples. Grain boundary shapes (GBS) noted in samples are: Cu (curved), Em (Embayed), Su (sutured), Str (straight).Accessory minerals are quartz (qtz), pyrite (py), graphite (gr), ferrous oxides and hydroxides (Fe-ox) and muscovite (ms). Minerals shown in brackets are present in extremely small amounts, whereas minerals in big letters are relatively abundant. Minerals mentioned with italics are trace minerals detected with SEM: apatite (ap), titanium dioxide (Ti-ox). Microcrystalline to cryptocrystalline calcite occurrence is marked as (m). Coarse grained veins (cv) show the typical size of vein constituent.